Journal of Proteomics 253 (2022) 104459

Contents lists available at ScienceDirect

Journal of Proteomics

journal homepage: www.elsevier.com/locate/jprot

Proteomic differences in apple spur buds from high and non-cropping trees during floral initiation

Julian Kofler [a,*], Anton Milyaev [a], Berit Würtz [b], Jens Pfannstiel [b], Henryk Flachowsky [c], Jens-Norbert Wünsche [a]

[a] Institute of Crop Science, Section of Crop Physiology of Specialty Crops (340f), University of Hohenheim, Emil-Wolff-Straße 23, 70599 Stuttgart, Germany
[b] Mass Spectometry Unit, Core Facility Hohenheim (640), University of Hohenheim, August-von-Hartmann-Str. 3, 70599 Stuttgart, Germany
[c] Institute for Breeding Research on Fruit Crops, Julius Kühn-Institut (JKI), Federal Research Centre for Cultivated Plants, Pillnitzer Platz 3a, 01326 Dresden, Germany

ARTICLE INFO

Keywords:
Alternate bearing
Flower induction
Malus ×domestica
Proteomic profiling

ABSTRACT

The cropping behavior of biennial apple (*Malus ×domestica* Borkh.) cultivars is irregular and often follows a biennial bearing pattern with 'On' years (high crop load and inhibited floral bud formation) followed by 'Off' years (little crop load and a promoted formation of floral buds). To study proteomic differences between floral and vegetative buds, trees of the strongly alternating cultivar 'Fuji' and the regular bearing cultivar 'Gala' were either completely thinned or not thinned at full bloom to establish two cropping treatments with no ('Off') or a high ('On') crop load, respectively. Student's *t*-Tests indicated significant differences of protein profiles in buds from 2-year old spurs from both treatments at each sampling date. Abundance patterns of protein clusters coincided with the onset of floral bud initiation and were most noticeable in buds from 'On' trees with a decreased abundance of key enzymes of the phenylpropanoid and flavonoid pathways and an increased abundance of histone deacetylase and ferritins. Furthermore, an increased abundance of proteins involved in histone and DNA methylation was found in the buds from 'Off' trees. This study presents the first large-scale, label-free proteomic profiling of floral and vegetative apple buds during the period of floral bud initiation.

Significance: Although several studies exist that address the complex developmental processes associated with the formation of floral buds in apple (*Malus ×domestica* Borkh.) at transcriptomic level, no data is available for explaining the difference between floral and vegetative buds or biennial and regular bearing cultivars on a proteomic level. This study presents the first large-scale, label-free proteomic profiling of floral and vegetative apple buds from the two cultivars 'Fuji' and 'Royal Gala' during the period of floral bud initiation and renders possible the development of suitable biomarkers for biennial bearing in apple.

1. Introduction

A crucial process in annual and perennial flowering plants is the development of floral meristems to enter the reproductive cycle and to ensure the formation of progenies. Proteins, steered by their respective transcripts or by interacting with other proteins, play an essential role in starting, conveying and executing floral development pathways. Prominent examples are the HEADING DATE 3a (Hd3a) protein acting as a mobile flowering signal in rice [1], the photoreceptor regulation of the CONSTANS (CO) protein in photoperiod-dependent flowering in *Arabidopsis thaliana* [2], the control of flowering time in *A. thaliana* through the spliceosome protein BAD RESPONSE TO REFRIGERATION 2 (BRR2) [3], the long-distance signaling of floral induction by FLOWERING LOCUS T (FT) protein movement in *A. thaliana* [4] or the repression of floral development by FT protein's close relative TERMINAL FLOWER 1 (TFL1) [5].

Apple (*Malus ×domestica* Borkh.) starts its 2-year reproductive cycle with the process of flower bud induction during early summer, when the vegetative meristems perceive an until now unknown signal that triggers floral bud development [6–9]. Apple flowers are predominantly formed in the terminal buds of short shoots, so-called spurs [9,10]. The first visible structural changes of the bud meristem appear during the second phase of floral bud development, termed floral bud initiation, when a pronounced doming and broadening of the bud apex appears [8,9,11]. Flower bud formation continues until autumn with the development of inflorescence primordia and floral organs. This third stage of flower bud

* Corresponding author.
E-mail address: julian.kofler@uni-hohenheim.de (J. Kofler).

https://doi.org/10.1016/j.jprot.2021.104459
Received 1 February 2021; Received in revised form 28 November 2021; Accepted 10 December 2021
Available online 17 December 2021

differentiation is then temporarily interrupted with the onset of bud dormancy and completed in the following spring shortly before bud burst with the formation of pollen sacs and ovules [12,13].

A major constraint of obtaining constant and thus economically viable yields in commercial apple orchards is the irregularity of cropping due to biennial bearing [14]. It is characterized by large yields of small-sized fruit in 'On' years and low yields of over-sized fruit in 'Off' years [15]. It is assumed that the competitive overlap of flower bud formation for the following season and fruit growth within the current season is the physiological reason for this cropping behavior [9,16,17]. However, the specific causal mechanism of how a fruit inhibits or the absence of a fruit promotes the development of the subtending spur bud still remains unclear. Although several studies exist that address this topic at transcriptomic level [18–20] with changes in DNA and/or histone methylation pattern [21,22], data or coherent models are not available for explaining the difference between 'On' and 'Off' or biennial and regular bearing apple cultivars at proteomic level.

In this study, apple spur buds were collected during one growing season from trees with heavy and no crop load of two cultivars differing in their bearing behavior, respectively. The proteomic profile of spur buds at different developmental stages was analyzed and cultivar differences were identified. As part of a larger transdisciplinary and multifocal project identifying the underlying mechanisms of biennial bearing in apple, this study focuses on the time-dependent proteomic changes in floral and vegetative apple spur buds in an attempt to contribute to a holistic understanding of the induction of flower buds in apple.

2. Material and methods

2.1. Experimental design and bud sampling

The experiment was conducted at the Centre of Competence for Fruit Cultivation near Ravensburg in Southern Germany. Two apple cultivars with a different degree of biennial bearing behavior were used: 'Fuji', clone 'Raku-Raku', known to be a strongly biennial bearing cultivar, and 'Gala', clone 'Galaxy', known as a more regular bearer. The experimental plot consisted of 130 'Fuji' and 'Gala' trees, respectively, each in two neighboring 65-tree rows next to one another. Half of the trees were completely flower thinned ('Off' trees) by hand at full bloom on 30 April 2015 (both cultivars), whereas the other half of the trees was not flower thinned and remained the high return bloom density ('On' trees). Setting up these extreme crop load treatments was done (i) to synchronize bud development within the trees to obtain homogenous bud samples from each trees, (ii) to increase flower bud induction in 'Off' trees and (iii) to inhibit flower bud induction in 'On' trees. Sampling started in the fourth week after full bloom (afb) and continued weekly for 15 weeks until 2 September 2015. At each sampling date, three randomly selected trees (one tree representing one biological replicate) per cultivar and treatment were selected and 55 buds from 2-year-old spurs were randomly sampled off each tree. During the sampling period, no tree was selected more than once. An overview of the experimental design and sampling procedure is given in Fig. 1.

Immediately thereafter, buds with their scales removed were snap-frozen in liquid nitrogen and stored in safe-lock tubes at −80 °C until further processing. The developmental stages of the buds were determined using histological analysis as described in detail [23]. From those results, eight continuous sampling dates were selected to cover the periods of flower bud induction and initiation in both cultivars, respectively, as shown in Fig. 2. Due to the different bud initiation starting point (Fig. 2), different sampling dates were selected for 'Fuji' and 'Gala'. For 'Fuji', samples from 34 to 83 days after full bloom (dafb) and for 'Gala' samples from 68 to 118 dafb were selected, respectively. This approach permitted cultivar comparison since floral bud development in 'Gala' started later than in 'Fuji' and in 'Gala' also crop load comparison [24].

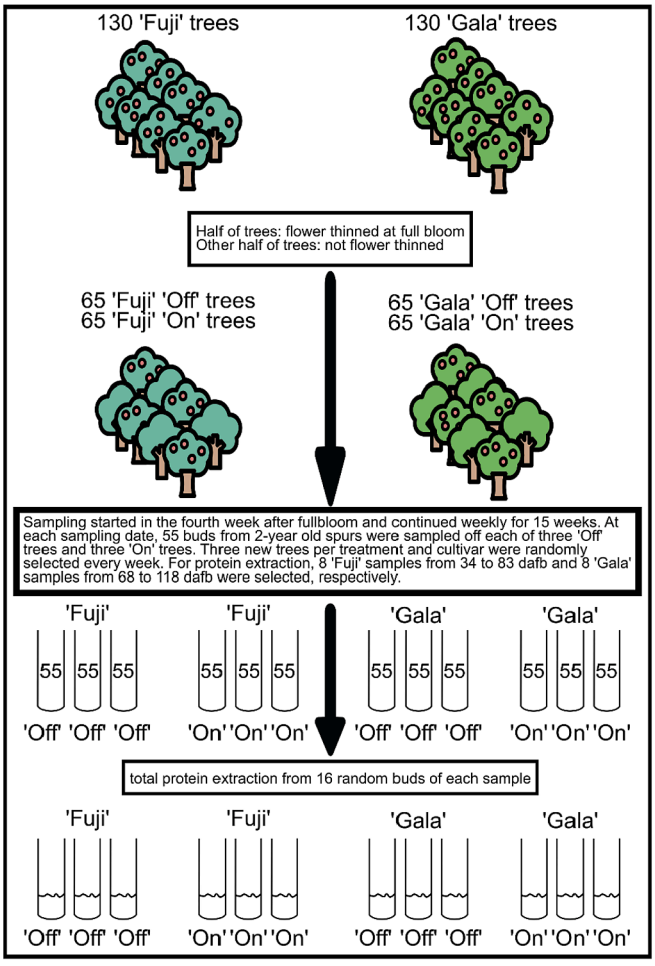

Fig. 1. Schematic workflow figure of experimental design, bud sampling and protein extraction.

2.2. Protein extraction

Sixteen buds per tree were pooled together constituting one biological replicate (600 mg fresh weight). The sixteen randomly selected buds were ground in a cryogenic mixer mill (CryoMill, Retsch GmbH, Haan, Germany) cooled with liquid nitrogen. To achieve a homogenous pulverization, four buds were put in one safe-lock tube with two stainless steel balls of 5 mm diameter and four safe-lock tubes were ground in two grinding cycles with each 3 min long at the frequency of 25 Hz. Immediately after grinding, 1.5 ml of freshly prepared lysis buffer (150 mM Tris-HCl, 2% sodium dodecyl sulfate, 20 mM dithiothreitol, adjusted to pH 6.8) was added to each safe-lock tube [25]. After shaking and 3 min incubation at room temperature, the milling balls were removed using a magnet and the samples were centrifuged for 8 min at 20,000 rcf. All four supernatants from one replicate were transferred into a single 15 ml conical centrifuge tube. An aliquot of 200 µl was transferred to a new 1.5 ml safe-lock tube (Eppendorf AG, Hamburg, Germany) for protein precipitation using chloroform/methanol [25] and the obtained protein pellet was stored in digestion buffer (6 M urea, 50 mM Tris-HCl pH 8.5) at 4 °C until further processing. Protein concentration was determined using the Bradford assay [26] and 25 µg of proteins were digested in-solution using a mixture of Trypsin (Roche Pharma AG, Basel, Switzerland) and Lys-C (Wako Chemical GmbH, Neuss, Germany) [27]. Peptides were desalted and purified using the C18-StageTips method [28] and resuspended in 20 µl of 0.1% trifluoroacetic acid (Sigma-Aldrich, St. Louis, USA). Four quality control samples were created, each representing a pooled sample of 24 out of 96 randomly drawn samples,

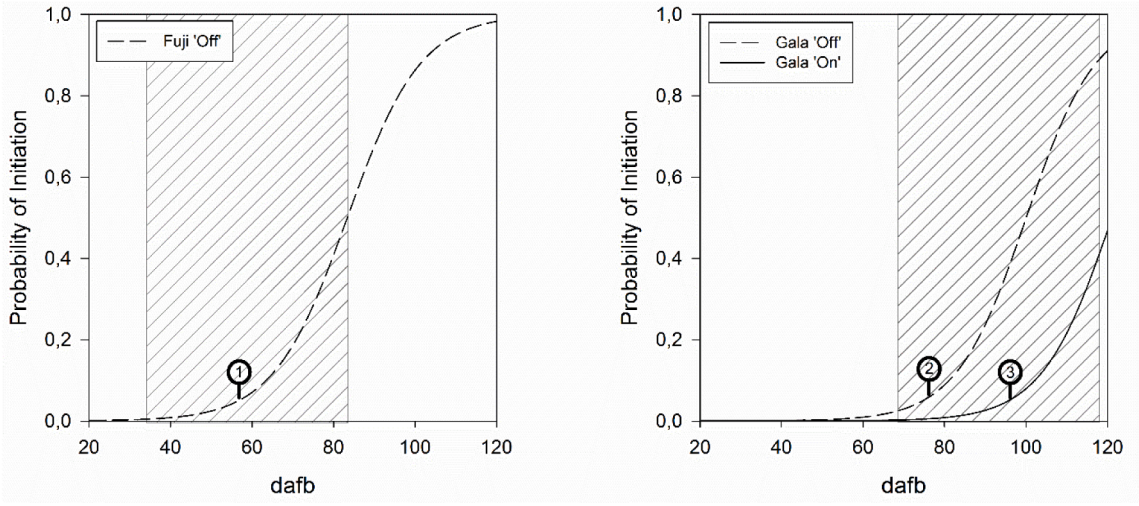

Fig. 2. Calculated prediction of flower bud initiation based on histological data [23]. Starting point of bud initiation for 'Fuji' 'Off' was 57 dafb (1), for 'Gala' 'Off' 76 dafb (2) and for 'Gala' 'On' 96 dafb (2), respectively. No starting point of bud initiation could be calculated for 'Fuji' 'On' due to a lack of initiated buds. Shaded area indicates the time window for proteomic profiling: 34 dafb to 83 dafb for 'Fuji' and 68 dafb to 118 dafb for 'Gala'.

resulting in 100 samples in total.

2.3. ESI-MS method

Nanoscale liquid chromatography electrospray ionization tandem mass spectrometry (Nano-LC-ESI-MS/MS) analysis was performed on an EASY-nLC 1000 system (Thermo Fisher Scientific, Waltham, USA) coupled to a Q-Exactive Plus mass spectrometer (Thermo Fisher Scientific, Waltham, USA), using an EASY-Spray nanoelectrospray ion source (Thermo Fisher Scientific, Waltham, USA), at the Core Facility Hohenheim, Mass Spectrometry Unit (University of Hohenheim, Stuttgart, Germany). Tryptic peptides were injected directly to an EASY-Spray analytical column (PepMap RSLC C18, 2 µm 100 Å 75 µm × 250 mm column, Thermo Fisher Scientific, Waltham, USA), operated at a constant temperature of 40 °C. Gradient elution was performed at a flow rate of 250 nl min^{-1} using two solvents. 0.5% acetic acid (solvent A) and 0.5% acetic acid in 80% acetonitrile (solvent B) during 140 min with the following gradient profile: equilibration with 10 µl of 3% solvent B, followed by a gradient of 3% - 10% of solvent B in 50 min, 10% - 22% solvent B in 40 min, 22% - 45% solvent B in 25 min, 45% - 95% solvent B in 10 min, 15 min isocratic at 95% solvent B. The mass spectrometer was operated using Xcalibur software (version 4.0.27, Thermo Fisher Scientific, Waltham, USA). Survey spectra ($m/z = 300–1600$) were detected in the Orbitrap at a resolution of 70,000 at $m/z = 200$. Data dependent tandem mass spectra were generated for the 10 most abundant peptide precursors in the Orbitrap. For all Orbitrap measurements, internal calibration was performed using lock-mass ions from ambient air [29].

2.4. Protein identification and statistics

MS data were analyzed using MaxQuant (version 1.6.2.10) [30] in the label-free quantification (LFQ) mode with carbamidomethylation of cysteine residues as fixed modification and oxidation of methionine and n-terminal acetylation as variable modifications. A maximum of three missed cleavages was allowed and the match between runs function was switched on. The peak list was searched against all 45,116 FASTA-formatted protein sequences from the GDDH13 apple genome version 1.1 [31].

LFQ intensities calculated by MaxQuant were loaded into Perseus (version 1.6.10) [32] for statistical analysis. Reverse hits, identifications only by site and potential contaminants were removed and LFQ intensities log2(x) transformed. The unique peptide threshold was set to the minimum of two and the valid values filter was set to a minimum of three valid values during at least one sampling date in at least one cultivar and treatment. Missing values were imputed with random numbers from the normal distribution and a down shift of 1.8 only to create the partial least-squares discriminant analysis (PLS-DA) which requires all data points to be present. PLS-DA was computed using MetaboAnalyst 5.0 [33]. A two-sided Student's *t*-Test between the treatments was performed separately for the cultivars ('Fuji' 'Off' vs. 'Fuji' 'On' and 'Gala' 'Off' vs. 'Gala' 'On') at each sampling date with 250 randomizations, the Benjamini and Hochberg false discovery rate (FDR) [34] of 0.01 and the bio-weight factor [35] as significance criteria by setting the S0 value to 0.01. No missing values were imputed for the Student's *t*-Tests. The number of degrees of freedom for the two samples Student's t-Tests was: $(n_1 + n_2)-2 = 4$ with $n_1 = 3$ and $n_2 = 3$. Only proteins that were significantly different between treatments during at least one sampling date were considered for further analysis. Intensities were then z-score normalized, where the mean of each row (protein) is subtracted from each value from that row (protein) and the result is divided by the standard deviation of the row. Hierarchical clustering was performed with Euclidean distance, linkage type average, preprocessing with k-means and a fixed cluster number of four. The mean value and standard error of all z-scored protein abundances belonging to one cluster was calculated at each date and plotted against dafb using SigmaPlot 12.3 (Systat Software Inc., San Jose, USA).

Protein sequences from the resulting eight clusters were blasted against the non-redundant NCBI protein sequence database with the specific taxonomy 3750 (*Malus ×domestica*) with word size 3 and a High Scoring Pairs (HSP) length cutoff of 33 using OmicsBox 1.2.4 (BioBam Bioinformatics S.L., Valencia, Spain) for annotation with descriptions, Gene Ontology terms (GO), InterPro GO terms and enzyme codes from the Kyoto Encyclopedia of Genes and Genomes (KEGG) [36] pathway database. Functional protein interaction analysis was done using STRING version 11.0 [37] by uploading multiple fasta-formatted amino acid sequences. As a reference organism, we chose *Arabidopsis thaliana* because preliminary functional analysis revealed that reference organisms such as *Malus ×domestica* or *Fragaria vesca* yielded less identified functional clusters and characterizations. Using the protein sequences from all eight clusters, the reference organisms *Malus ×domestica* and *F. vesca* resulted only in 42 and 41 functional clusters, respectively, whereas *A. thaliana* resulted in 52 functional clusters. Functional annotation clustering was done using the MCL algorithm with an inflation parameter of three [38].

3. Results and discussion

In total, 7194 different proteins were identified in our proteomics experiment. The average count of peptides per sample prior to all filtering steps was 41,699, the average count of unique peptides was 17,115 and the average count of identified proteins was 3970. 6025 proteins corresponding to 13.4% of the total apple proteome [31] remained after removing all proteins with less than two unique peptides. Subsequently, all proteins were discarded that did not fulfill the criteria of having three LFQ values in at least one cultivar-date-treatment combination. 4020 proteins remained for further analysis corresponding to 8.9% of the total apple proteome (Annex 3).

As shown in Fig. 3, the PLS-DA shows variation between samples with two main components explaining 17.1% of the variance. The quality control samples cluster next to each other, indicating high reproducibility of sample preparation and subsequent Nano-LC-MS/MS analysis. While a basic separation between cultivars could be observed, the PLS-DA was not able to differentiate clearly between treatments. This might be explained by two factors that cause variability among bud samples. First, bud development underlies a certain within-tree heterogeneity, which leads to the circumstance that a random sample of collected buds from one tree at a certain time always includes buds that are differentially progressed in their development [39]. Second, a certain biologically expected variability is also observed between trees of the same cultivar in the same field [40].

The results of global Student's *t*-Tests between treatments within each cultivar are shown in Fig. 4. A marked difference of the abundance of proteins between the two treatments shows that two different developmental pathways have been triggered.

3.1. Cultivar 'Fuji'

The Student's t-Tests performed at each sampling date resulted in 159 proteins that were significantly different in abundance between samples from 'Fuji' 'On' and 'Off' trees during at least one sampling date while 17 out of 159 were significantly different at two sampling dates. 93 were higher abundant in buds from 'On' trees and 66 were higher abundant in buds from 'Off' trees. Overall, significant treatment differences in abundance of protein species existed with one protein at 34 dafb, 23 proteins at 62 dafb, 31 proteins at 68 dafb and 121 proteins at 75 dafb. The z-scores of the following clusters represent the mean z-scores of all protein abundances belonging to the various clusters. Clusters 46, 90 and 155 consist of proteins that are more abundant in buds from 'On' trees, whereas cluster 132 consists of proteins that are more abundant in buds from 'Off' trees. Cluster analysis presents four clusters of protein species, showing distinct abundance profiles over time (Fig. 5).

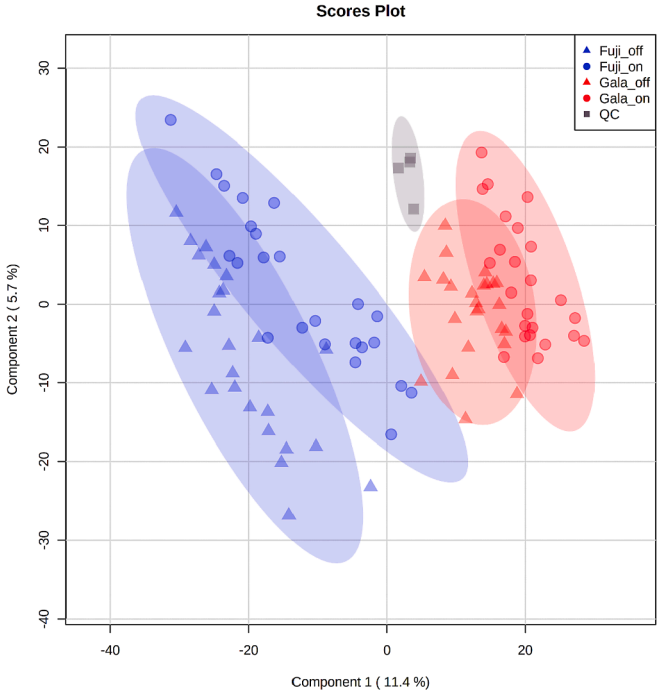

Fig. 3. PLS-DA of all samples including quality control samples (QC). Missing values were imputed with random numbers from the normal distribution. Blue: 'Fuji'; red: 'Gala'; grey: QC; triangular: 'Off'; circle: 'On'; square: QC. Filled ellipses: 95% confidence region. (For interpretation of the references to colour in this figure legend, the reader is referred to the web version of this article.)

Cluster 132, containing 43 proteins, was more abundant in buds from 'Off' trees than those from 'On' trees throughout the entire experimental period with a mean log2FC of −1.4 and a pronounced treatment separation starting shortly after the onset of bud initiation (Fig. 5). The decrease in buds from 'On' trees, which were mostly vegetative buds, during the onset of bud initiation might indicate that this cluster consists of proteins that advance floral bud development. MADS-box proteins and other transcription factors related to flowering could not be identified with the exemption of a K-box region and MADS-box transcription factor family protein (MD09G1009100). However, the protein was not identified in enough samples to perform a statistical analysis. Similar difficulties were observed also in a proteomics study on transcription factors involved in the regulation of flowering in *Adonis amurensis* [41]. The protein with the highest log2FC in cluster 132 was a caffeoyl-CoA 3-*O*-methyltransferase (MD13G1117900, EC:2.1.1.267, F:GO:0008171) that significantly differed at 68 and 75 dafb with a log2FC of −2.47. The protein is part of the flavone and flavonol biosynthesis pathway (ec00944) where it catalyzes the synthesis of the flavonols Laricitrin and Syringetin [36] and was also found to be involved in the initiation of bud dormancy-release in *Pinus sylvestris* [42]. STRING analysis of cluster 132 shows six functional clusters. The largest functional cluster with six proteins includes two S-adenosylmethionine synthetases (SAMS), SAM1 and SAM2, that catalyze S-adenosylmethionine. In rice, SAMS is essential for histone and DNA methylation to regulate gene expression related to flowering as the knockdown of SAMS genes resulted in late flowering phenotypes [43]. The phenylalanine ammonia-lyase (PAL1), the key enzyme of the phenylpropanoid pathway [44], was at the center of a cluster belonging to the phenylpropanoid and flavonoid biosynthetic process. PAL1 was accompanied by Naringenin,2-oxoglutarate 3-dioxygenase (F3H), an intermediate in the biosynthesis of flavonols, which is possibly related to the synthesis of Naringenin and was shown to accumulate during the onset of dormancy in peach buds [45]. Part of the cluster is also LDOX, a leucoanthocyanidin dioxygenase associated to the phenylpropanoid pathway synthesizing anthocyanin [46] and a putative caffeoyl-CoA *O*-methyltransferase (CCOAMT).

Cluster 155 contains 24 proteins with an average log2FC of −0.31; however, there was no treatment related difference in abundance during the period of bud initiation (Fig. 5). The protein with the highest log2FC in cluster 155 was calmodulin (MD14G1241000, P:calcium-mediated signaling; F:calcium ion binding) that was significantly different at 75 dafb with a log2FC of −3.17. Calmodulin is the predominant calcium receptor in eukaryotes and essential for the Ca^{2+}/calmodulin-mediated signal network in plants [47]. STRING analysis of cluster 155 resulted in three functional clusters. However, no relevant functions related to bud development could be attributed to the proteins of cluster 155, as expected by the similar abundances of the protein clusters in 'On' and 'Off' buds.

Cluster 46, containing 47 proteins with an average log2FC of 1.4 was more abundant in buds from 'On' trees than those from 'Off' trees with a significant difference at 75 dafb (Fig. 5). Consequently, proteins belonging to cluster 46 could be involved in vegetative growth. The protein with the highest log2FC in cluster 46 is a plasma membrane intrinsic protein, probably aquaporin PIP2 (MD07G1174700, P:

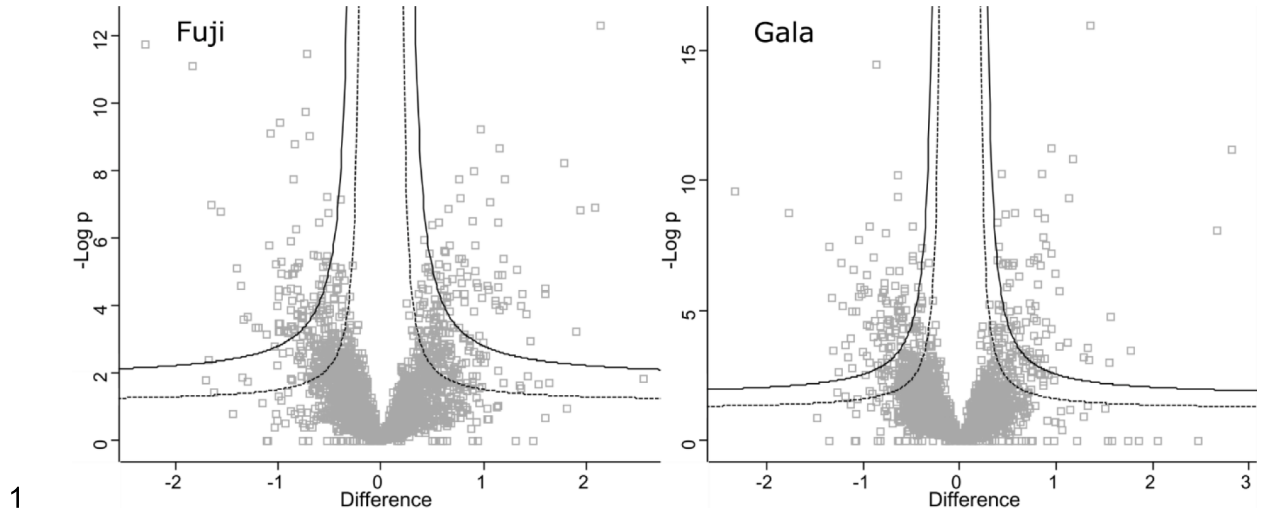

Fig. 4. Volcano plots showing the difference in log2FC of protein abundance in buds from 'On' and 'Off' trees for the cultivars 'Fuji' and 'Gala'. Each square represents the relative abundance of one protein species. Positive differences refer to a higher abundance in buds from 'On' trees, negative differences refer to higher abundance in buds from 'Off' trees. Solid line represents class A significance criteria with FDR = 0.01 while the dashed line represents class B significance criteria with FDR = 0.05.

transmembrane transport; F:channel activity; C:membrane), with a log2FC of 2.49. STRING analysis of cluster 46 shows seven functional clusters mainly associated with responses to abiotic stimuli such as light and temperature and immune responses to pathogens. Six proteins that were more abundant in buds from 'On' trees than those from 'Off' trees at 75 dafb belong to the photosystem one and photosystem two oxygen evolving complex (LHCA3, LHCA4, LHCA5, CAB1, DRT112 and AT4G01150) located in the thylakoids.

Cluster 90 contains 45 proteins with an average log2FC of 1.5 and showed an increasing abundance in 'Fuji' 'On' buds throughout the experimental period with the highest number of significant hits (38) at 75 dafb (Fig. 5). There was a clear difference between buds from 'On' and 'Off' trees, starting to become pronounced at 48 dafb, 9 days prior to the calculated onset of bud initiation at 62 dafb [23]. The protein with the highest log2FC in cluster 90 was an uncharacterized protein (MD09G1119300) with log2FC of 2.64. It shows sequence similarity to the fruit protein pKIWI501 from *Pyrus bretschneideri* (mean similarity 75.25%) and also to the cytochrome *c*1 from *Prunus dulcis* (Similarity 56.3%). STRING analysis of cluster 90 shows five functional clusters. At the center of a cluster with seven proteins is ferretin-1 (FER1). Loss of ferritins resulted in a reduced growth and strong defects in flower development in *Arabidopsis thaliana* [48]. Hence, the increase of ferritin-1 in 'Fuji' 'On' buds possibly promotes growth of vegetative buds. Another cluster with seven proteins consists of granule-bound starch synthase 1 (GBSS1) that is required for the synthesis of amylose and alpha-galactosidase 2 (AGAL2), which has an essential function during leaf development in *A. thaliana* [49] indicating a possible involvement in vegetative growth. This is supported by the increase of abundance of cluster 90 in buds from 'On' trees. There is also a cluster with two proteins belonging to the small interfering RNA (siRNA) biogenesis: AT2G37020.2, a translin family protein, and AGO4, an argonaute family protein that directs chromatin modifications, including histone methylation and DNA methylation [50].

Table 1 shows the top 20 proteins that have the highest (more abundant in buds from 'On' trees) and lowest (more abundant in buds from 'Off' trees) log2FC for the cultivar 'Fuji', respectively.

3.2. Cultivar 'Gala'

The Student's t-Tests performed at each sampling date resulted in 53 proteins that were significantly different in abundance between bud samples from 'Gala' 'On' and 'Off' trees during at least one sampling date, whereas this was the case for one protein at two sampling dates (Table 2 and Annex 1). Fourteen were higher abundant in buds from 'On' trees and 39 were higher abundant in buds from 'Off' trees. Overall, significant treatment differences in abundance of proteins existed with 27 proteins at 83 dafb, one protein at 89 dafb and at 97 dafb, respectively, 21 proteins at 104 dafb and 4 proteins at 118 dafb. Cluster analysis presents four clusters of protein species, showing distinct time-dependent abundance profiles (Fig. 6). Cluster 22 and 37 consisted of proteins that were more abundant in buds from 'Off' trees, meaning that those proteins could possibly be involved in floral bud development, whereas cluster 45 and cluster 49 consisted of proteins that were more abundant in buds from 'On' trees and possibly be involved in promoting vegetative growth.

Cluster 22 contains 23 proteins that were more abundant at all sampling points in buds from 'Gala' 'Off' trees than those from 'On' trees with an average log2FC of −1.66 (Fig. 6). The abundance stayed relatively constant in buds from 'Off' trees but was more inconsistent with a noticeable decrease at 83 dafb and 104 dafb in buds from 'On' trees. The protein with the highest log2FC in cluster 22 was the caffeoyl-CoA 3-*O*-methyltransferase (MD13G1117900, EC:2.1.1.104) with log2FC of −3.13 at 118 dafb. This protein is part of the phenylpropanoid and flavonoid biosynthesis pathways [36] and reported to be involved in the biosynthesis of lignin [51]. STRING analysis of cluster 22 shows five functional clusters. The largest, with five proteins, is similar to cluster 132 in 'Fuji' and includes key enzymes of the phenylpropanoid and flavonoid biosynthetic process: PAL1, F3H, LDOX, CCOAMT and additionally trans-cinnamate 4-monooxygenase (C4H) that synthesizes p-coumaric acid in the phenylpropanoid pathway [52]. Furthermore, the FDM2/IDN2 complex found in cluster 22 is required for gene silencing by RNA [53].

Cluster 37 contains 16 proteins with an average log2FC of −1.7 and was always more abundant in buds from 'Gala' 'Off' than those from 'On' trees (Fig. 6). The abundance decreased distinctly in 'On' trees at 83 dafb, recovered until 97 dafb when it continuously declined toward the last sampling date. The protein with the highest log2FC in cluster 37 is the eukaryotic translation initiation factor 3 subunit F-like (MD01G1148100, P:translational initiation; F:translation initiation factor activity) with a log2FC of −2.7 at 83 dafb, which was shown to be required for embryogenesis and cell differentiation in *A. thaliana* [54]. STRING analysis of cluster 37 shows three functional clusters. The largest cluster with five proteins is a photosynthesis cluster with no relation to flower bud development. One cluster has the translation

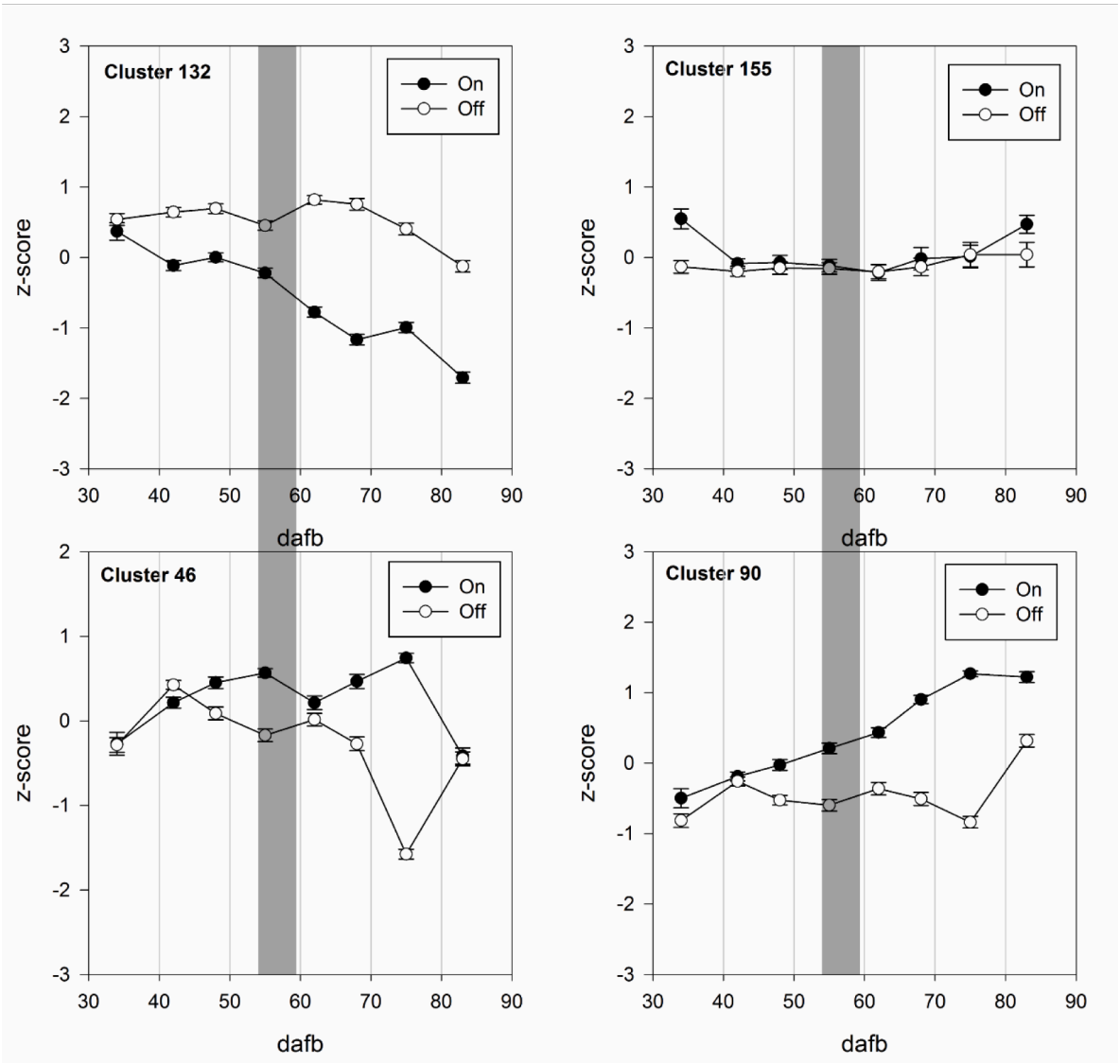

Fig. 5. Normalized means of relative protein abundances from each cluster in buds from 'Fuji' 'On' and 'Off' trees. All proteins that were used for hierarchical clustering showed a significant difference between 'On' and 'Off' during at least one time point at FDR = 0.01. Error bars indicate standard error of z-score. Grey bar indicates onset of bud initiation for 'Fuji' 'Off' at 57 dafb as identified by histological analysis [23]. Cluster 132: $n = 43$; cluster 155: $n = 24$; cluster 46: $n = 47$; cluster 90: $n = 45$.

initiation factors EIF2 and EIF4A-2, which are involved in cell growth and differentiation during embryogenesis [54]. There is also a cluster of two proteins involved in the methionine biosynthetic process (ATMS1 and AKHSDH2) that could be involved in the same process as the two SAMS from the 'Fuji' cluster 132, which has a similar abundance in 'On' and 'Off' buds.

Cluster 45 contains 9 proteins with an average log2FC of 1.9 and had a steadily increasing abundance in 'Gala' 'On' buds during the eight sampling dates (Fig. 6), indicating that those proteins are possibly involved in vegetative bud growth. The separation between 'On' and 'Off' buds was occurring from the first sampling date, and prior to the calculated onset of bud initiation [23] at 76 dafb. The protein with the highest log2FC is ferritin-4 (MD12G1178500, P:iron ion transport; P: cellular iron ion homeostasis; F:ferric iron binding) with a log2FC of 4.09 at 118 dafb. Similar to FER1 in cluster 90 in 'Fuji', the increase of ferritin-4 in 'Gala' 'On' buds possibly promotes growth of vegetative buds [48]. No functional clusters could be identified using STRING analysis.

Cluster 49 contains 5 proteins with an average log2FC of 1.52 and showed minor treatment differences throughout the observation period, except for a pronounced increase in 'On' buds at 83 dafb (Fig. 6) indicating a possible involvement in vegetative bud growth. The highest log2FC (2.13) contained in cluster 49 was found at 104 dafb and is related to a class 1 heat shock protein (MD17G1020300). However, the protein with the highest log2FC (1.9) at 83 dafb was a histone deacetylase (MD11G1156500). Histone deacetylases are reported to regulate flowering time in *A. thaliana*, where the lack of histone deacetylases leads to a hyperacetylation of histones in the chromatin of the floral repressor FLC and thus up-regulation of FLC and delayed flowering [55]. RNA of this protein was also reported to be upregulated in terminal buds from 'On' trees as early as 30 dafb in another study [21]. Histone deacetylases are also reported to be associated with breaking seed dormancy in *A. thaliana* [56]. It could be assumed, that histone deacetylase has a vegetative growth inducing effect and initiates the growth of vegetative buds. Furthermore, histone deacetylases are often linked with transcriptional repression [57], which may result in an inhibiting effect on floral initiation. The time point also coincides with the marked decrease of cluster 37 in 'On' buds, containing the eukaryotic translation initiation factor 3 (MD01G1148100), which was shown to be required for cell differentiation in *A. thaliana* [54]. No functional clusters could be

Table 1
The 40 key proteins with the highest log2FC between bud samples from 'Fuji' 'On' and 'Off' trees with corresponding GDDH13 ID, description, gene symbol, indication at which sampling date the difference was significant at FDR = 0.01, *p*-value, log2FC 'On' over 'Off', count of unique peptides per protein, cluster affiliation and biological process. 40 shown out of 159 (Annex 1).

ID	Description	Gene symbol	dafb*	-log (p)	log2FC On-Off	Unique peptides	Cluster	GO Biological process
MD09G1119300	fruit protein pKIWI501	LOC103411284	62, 68	2.64	3.67	14	90	
MD09G1267600	embryonic protein DC-8-like	LOC103444213	62, 68	3.47	3.14	21	90	
MD08G1067400	aminopeptidase M1-like	LOC103440784	75	2.55	3.13	12	90	P:proteolysis
MD06G1122100	granule-bound starch synthase 1, chloroplastic/amyloplastic-like	LOC103437450	75	2.36	2.72	10	90	
MD12G1178500	ferritin-4, chloroplastic-like	LOC103430428	68, 75	2.74	2.56	9	90	P:iron ion transport; P:cellular iron ion homeostasis
MD07G1174700	plasma membrane intrinsic protein subtype 2 aquaporin	LOC103428693	68, 75	2.59	2.49	4	46	P:transmembrane transport
MD09G1081400	probable endo-1,3(4)-beta-glucanase ARB_01444	LOC103425953	62, 75	2.53	2.27	13	90	
MD05G1319100	polyphenol oxidase	LOC103408840	75	3.63	2.27	6	90	P:pigment biosynthetic process; P: oxidation-reduction process
MD11G1133400	beta-galactosidase 8	LOC103430004	75	2.71	2.17	7	90	P:carbohydrate metabolic process
MD08G1244100	elongation factor 1-gamma	LOC103442035	75	2.80	2.10	12	46	P:translational elongation
MD06G1195000	chlorophyll *a*-b binding protein P4, chloroplastic	LOC103437829	75	2.20	2.10	2	46	P:photosynthesis, light harvesting
MD06G1169400	small nuclear ribonucleoprotein-associated protein B′-like	LOC103419552	75	2.87	2.08	6	46	P:mRNA splicing, via spliceosome
MD00G1060100	pre-mRNA-processing factor 39 isoform X1	LOC103435758	75	2.28	2.05	15	46	
MD15G1223500	sucrose synthase	LOC103400901	75	2.27	2.05	18	46	P:sucrose metabolic process
MD09G1054700	uncharacterized protein At5g39570-like	LOC103416997	75	2.23	1.99	20	46	
MD01G1199000	3-hexulose-6-phosphate isomerase	LOC103440558	75	2.23	1.95	5	90	
MD09G1011300	sulfite oxidase	—NA—	75	3.24	1.93	9	90	P:oxidation-reduction process
MD15G1044000	aspartyl protease family protein At5g10770-like	LOC103442424	75	2.37	1.93	13	46	P:proteolysis
MD06G1008700	catalase isozyme 1	LOC103412102	75	2.45	1.93	37	90	P:response to oxidative stress; P: oxidation-reduction process
MD14G1188600	protein EDS1L-like	LOC103415247	75	2.15	1.92	44	46	P:lipid metabolic process
MD10G1009700	ATP phosphoribosyltransferase 1, chloroplastic-like	LOC103429431	62	3.39	−1.58	7	132	P:histidine biosynthetic process
MD11G1143300	UDP-glucuronic acid decarboxylase 6 isoform X1	LOC103412987	62	3.01	−1.60	14	132	P:D-xylose metabolic process
MD15G1372600	phospho-2-dehydro-3-deoxyheptonate aldolase 1, chloroplastic-like	LOC103419477	68	3.60	−1.62	5	132	P:aromatic amino acid family biosynthetic process
MD17G1283400	S-adenosylmethionine synthase 1	LOC103405960	62	2.96	−1.64	8	132	P:S-adenosylmethionine biosynthetic process
MD11G1241700	protochlorophyllide reductase, chloroplastic	LOC103408017	68	3.12	−1.65	23	132	P:oxidation-reduction process
MD07G1228300	biotin carboxyl carrier protein of acetyl-CoA carboxylase 2	LOC103432877	62	2.85	−1.68	5	155	
MD14G1010800	NADH–cytochrome *b*5 reductase 1	LOC103430924	68	2.84	−1.75	5	132	P:oxidation-reduction process
MD05G1168200	chloroplast envelope quinone oxidoreductase homolog	LOC103435884	62, 68	3.35	−1.86	3	132	P:oxidation-reduction process
MD00G1040900	inositol-3-phosphate synthase	LOC103436971	62	3.76	−1.87	10	132	P:inositol biosynthetic process; P: phospholipid biosynthetic process
MD14G1092700	calmodulin-7-like isoform X2	LOC103410125	75	4.12	−1.87	13	155	P:calcium-mediated signaling
MD12G1187100	lipid transfer protein precursor	LOC103413913	75	2.47	−1.88	10	155	P:lipid transport
MD16G1160000	major allergen Mal d 1-like	LOC103423967	75	3.38	−1.90	3	132	P:defense response; P:abscisic acid-activated signaling pathway
MD07G1174800	caffeoylshikimate esterase-like	LOC103421001	68	3.36	−2.10	5	132	F:lipase activity
MD16G1120100	non-specific lipid transfer protein GPI-anchored 1	LOC103403172	75	2.23	−2.20	8	132	P:lipid transport; P:cuticle development; P:defense response to fungus
MD08G1097300	ribosome-inactivating protein	LOC103421128	62	3.50	−2.28	26	132	P:negative regulation of translation
MD16G1208600	40S ribosomal protein S15–4	LOC103408664	75	2.59	−2.40	2	155	P:translation
MD03G1290700	bifunctional epoxide hydrolase 2	LOC103419147	62	3.26	−2.43	3	132	
MD13G1160700	major allergen Pru av. 1-like	LOC103423965	62, 75	2.93	−2.45	5	132	P:defense response; P:abscisic acid-activated signaling pathway
MD13G1117900	flavonoid 3′,5′-methyltransferase-like isoform X1	LOC103403159	68, 75	2.90	−2.47	12	132	
MD14G1241000	calmodulin	LOC103403961	75	2.95	−3.17	5	155	P:calcium-mediated signaling

identified using STRING analysis.

Table 2 shows the top 20 proteins that have the highest (more abundant in buds from 'On' trees) and lowest (more abundant in buds from 'Off' trees) log2FC for the cultivar 'Gala', respectively.

3.3. Comparison between cultivars

As shown in Fig. 7, the correlation coefficients between the proteomic profiles of buds from 'On' and 'Off' trees decrease markedly after the

Table 2
The 40 key proteins with the highest log2FC between bud samples from 'Gala' 'On' and 'Off' trees with corresponding GDDH13 ID, description, gene symbol, indication at which sampling date the difference was significant at FDR = 0.01, *p*-value, log2FC 'On' over 'Off', count of unique peptides per protein, cluster affiliation and biological process. 40 shown out of 53 (Annex 1).

ID	Description	Gene symbol	dafb*	-log (p)	log2FC on-off	Unique peptides	Cluster	GO Biological process
MD12G1178500	ferritin-4, chloroplastic-like	LOC103430428	118	3.25	4.10	9	45	P:iron ion transport; P:cellular iron ion homeostasis
MD07G1268800	low-temperature-induced 65 kDa protein-like	LOC103439750	104	3.46	2.62	16	45	P:response to abscisic acid
MD02G1140000	cold-shock protein CS120-like	LOC103401165	104	2.85	2.49	21	45	P:response to water
MD17G1020300	class I heat shock protein-like	LOC103442187	104	3.97	2.13	6	49	
MD11G1156500	histone deacetylase HDT1-like	LOC103448002	83	4.60	1.96	5	49	
MD03G1164800	dihydropyrimidinase	—NA—	83	3.08	1.94	18	45	
MD02G1140100	cold-shock protein CS120-like	LOC103407093	104	3.53	1.68	21	45	P:response to water
MD11G1070800	asparagine synthetase [glutamine-hydrolyzing]	LOC103406611	89	3.58	1.55	26	45	P:asparagine biosynthetic process
MD14G1152400	protein DEK-like isoform X2	LOC103437514	83	3.66	1.55	3	49	P:regulation of double-strand break repair
MD13G1161400	major allergen mal d 1	LOC103403705	104	2.93	1.53	21	45	P:defense response; P:abscisic acid-activated signaling pathway
MD15G1294800	formamidase-like isoform X1	LOC103401494	104	3.54	1.47	25	45	
MD13G1078800	hypersensitive-induced response protein 2	LOC103451866	83	3.57	1.04	5	49	P:protein phosphorylation
MD10G1123700	protein EARLY-RESPONSIVE TO DEHYDRATION 7, chloroplastic-like	LOC103426994	104	4.35	1.02	23	45	
MD10G1076300	NADH dehydrogenase [ubiquinone] iron-sulfur protein 8, mitochondrial	LOC103440407	83	4.25	0.99	3	49	P:oxidation-reduction process
MD02G1207300	3-phosphoshikimate 1-carboxyvinyl-transferase 2	LOC103428057	104	4.32	−0.75	8	22	P:aromatic amino acid family biosynthetic process
MD12G1033000	3-oxoacyl-[acyl-carrier-protein] synthase III, chloroplastic-like	LOC103410834	104	4.40	−0.77	11	22	P:fatty acid biosynthetic process
MD06G1136900	glutamate-1-semialdehyde 2,1-amino-mutase 2, chloroplastic-like	LOC103437511	83	4.37	−1.04	10	22	P:tetrapyrrole biosynthetic process
MD17G1014700	protoporphyrinogen oxidase, mitochondrial-like	LOC103416942	104	4.16	−1.12	7	22	P:porphyrin-containing compound biosynthetic process; P:oxidation-reduction process
MD14G1022700	cytochrome *b*-c1 complex subunit 9-like	LOC103401874	83	3.68	−1.14	7	37	P:mitochondrial electron transport, ubiquinol to cytochrome *c*
MD06G1106100	long chain acyl-CoA synthetase 4-like	LOC103428271	83	3.46	−1.17	13	37	
MD04G1204000	probable linoleate 9S-lipoxygenase 5	LOC103433945	104	2.89	−1.62	27	37	P:oxidation-reduction process
MD11G1310700	serine/arginine-rich-splicing factor SR34-like	LOC103432664	83	3.17	−1.63	11	37	
MD06G1226100	uncharacterized protein LOC114825419	LOC103424564	83	3.20	−1.64	5	22	
MD11G1052900	trans-cinnamate 4-monooxygenase	LOC103418775	83, 104	3.49	−1.69	15	22	P:oxidation-reduction process
MD15G1246200	protein DMR6-LIKE OXYGENASE 2-like	LOC103436139	104	4.04	−1.72	7	22	P:oxidation-reduction process
MD08G1162600	photosystem II 22 kDa protein, chloroplastic	LOC103441569	83	2.98	−1.73	4	37	
MD05G1003800	bifunctional aspartokinase/ homoserine dehydrogenase 1, chloroplastic-like isoform X1	LOC103425227	83	2.97	−1.75	16	37	P:cellular amino acid biosynthetic process; P:oxidation-reduction process
MD06G1071600	anthocyanidin synthase	LOC103420259	104	3.62	−1.75	2	22	P:oxidation-reduction process
MD17G1003500	glyceraldehyde-3-phosphate dehydrogenase A, chloroplastic	LOC103425757	83	2.92	−1.75	2	37	P:glucose metabolic process; P: oxidation-reduction process
MD10G1009800	nuclear pore complex protein NUP160	LOC103403414	83	3.09	−1.79	10	37	P:nucleocytoplasmic transport
MD02G1282900	dynamin-related protein 4C-like	LOC103407440	104	3.30	−1.82	25	22	
MD04G1173600	lipid transfer protein precursor	LOC103453594	97	3.85	−1.89	6	22	P:lipid transport
MD03G1067100	internal alternative NAD(*P*)H-ubiquinone oxidoreductase A1, mitochondrial-like	LOC103406656	83	3.13	−2.02	7	37	P:oxidation-reduction process
MD07G1068700	cytochrome P450 89A2-like	LOC103438806	118	3.12	−2.07	14	37	P:oxidation-reduction process
MD05G1168200	chloroplast envelope quinone oxidoreductase homolog	LOC103435884	83	3.24	−2.31	3	22	P:oxidation-reduction process
MD11G1295100	ATP synthase CF1 beta subunit	LOC103450227	83	2.73	−2.41	8	37	P:ATP metabolic process; P:proton transmembrane transport
MD05G1259200	photosystem I reaction center subunit III, chloroplastic	LOC103423489	83	2.68	−2.46	2	37	P:photosynthesis
MD16G1201400	ATP sulfurylase 1, chloroplastic	LOC103403953	118	3.35	−2.63	13	22	P:sulfate assimilation
MD01G1148100	eukaryotic translation initiation factor 3 subunit F-like	LOC103455111	83	3.75	−2.70	3	37	P:translational initiation
MD13G1117900	probable caffeoyl-CoA *O*-methyltransferase At4g26220	LOC103403159	118	2.89	−3.13	12	22	

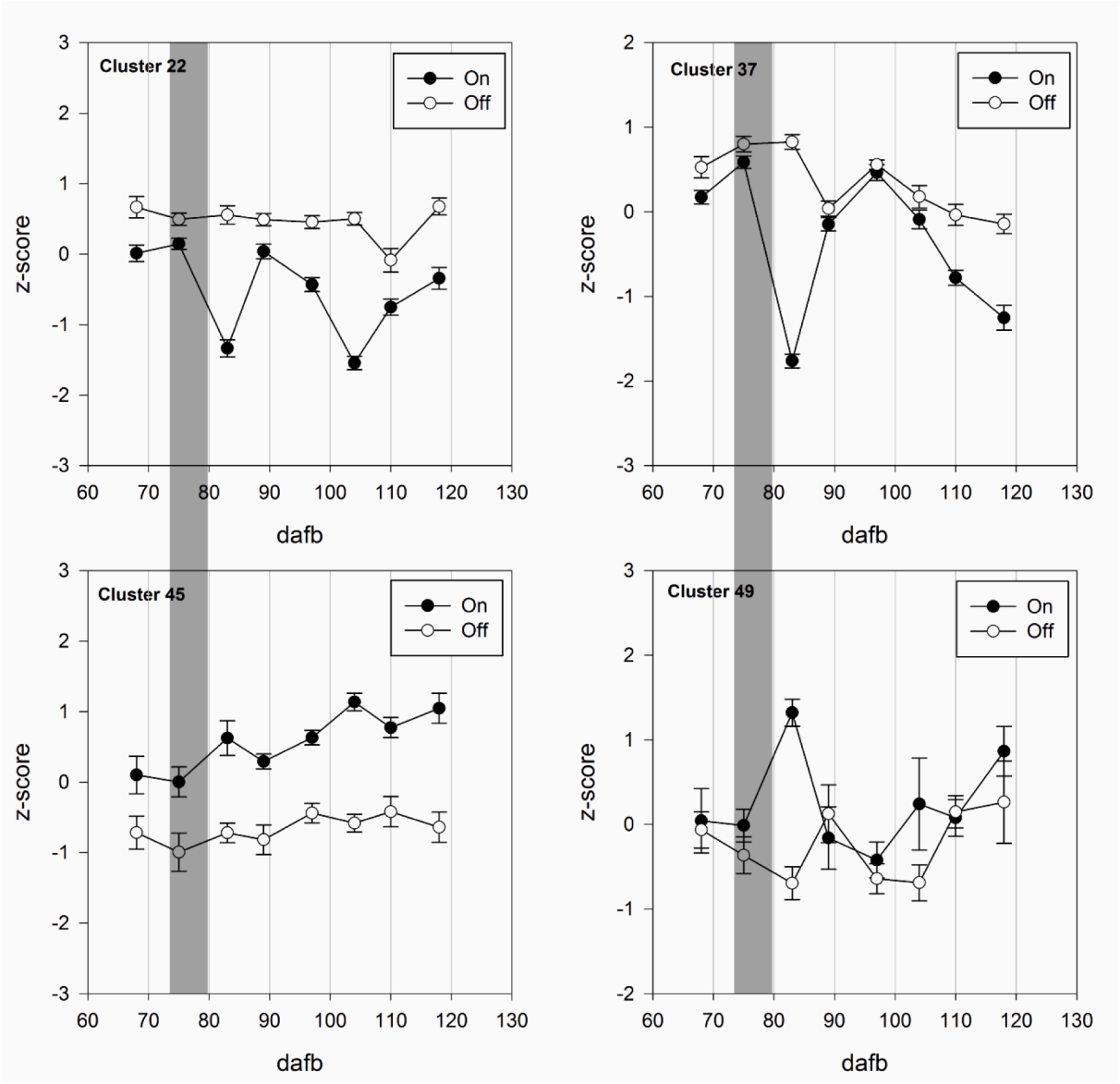

Fig. 6. Normalized means of relative protein abundances from each cluster in buds from 'Gala' 'On' and 'Off' trees. All proteins that were used for hierarchical clustering showed a significant difference between 'On' and 'Off' during at least one time point at FDR = 0.01. Error bars indicate standard error of z-scores. Grey bar indicates onset of bud initiation for 'Gala' 'Off' at 76 dafb as identified by histological analysis [23]. Cluster 22: $n = 23$; cluster 37: $n = 16$; cluster 45: $n = 9$; cluster 49: $n = 5$.

calculated onset of bud initiation in 'Off' trees. The decrease in 'Gala' coincides with the postponed calculated onset, confirming the later onset on a proteomic level.

As the floral bud development in 'Gala' trees begins later than in 'Fuji' trees, samples from different sampling points were compared. According to histological analysis [23], onset of bud initiation in 'Fuji' 'Off' was at 57 dafb and in 'Gala' 'Off' at 76 dafb. In order to compare cultivar differences, it was decided to compare samples from the sampling dates prior to the calculated onset of bud initiation. Therefore, the 'Off' samples from 55 dafb were selected from 'Fuji' and from 75 dafb from 'Gala', respectively. The Venn diagram in Fig. 8 shows the occurrence of similar and exclusive proteins in each cultivar.

A Student's *t*-Test, identical to the tests in chapter 3.1 and 3.2, between the two groups showed eighty-nine proteins that were significantly different abundant (Annex 2). 27 proteins were higher abundant in buds from 'Fuji' 'Off' trees, whereas 62 proteins were higher abundant in buds from 'Gala' 'Off' trees.

STRING analysis of the 27 proteins that were higher abundant in 'Fuji' than in 'Gala', identified a functional cluster consisting of flavone 3'-*O*-methyltransferase 1 (AT5G54160.1, OMT1), dihydroflavonol reductase (AT5G42800.1, DFR) and a putative caffeoyl-CoA *O*-methyltransferase (AT1G67980.1, CCOAMT). Another functional cluster contained the 60S ribosomal protein L13 (AT3G49010.3, BBC1), ribosomal protein L4/L1 (AT3G09630.1) and the 60S ribosomal protein L3–2 (AT1G61580.1, RPL3B) indicating higher translational activity in the bud meristems from 'Fuji' 'Off' trees. Furthermore, an uncharacterized protein was found to be higher abundant in buds from 'Fuji' trees: MD09G1079600, which has an 83% sequence similarity to a late embryogenesis abundant (LEA) protein from *Pyrus ussuriensis x Pyrus communis* (KAB2634038.1). LEA proteins are involved in seed maturation [58], which could indicate an early beginning of the floral bud development in 'Fuji' 'Off'. STRING analysis of the 62 proteins that were higher abundant in 'Gala' 'On' trees showed primarily a cluster of seven heat shock proteins and a cluster of three glutathione s-transferases that could not be attributed to any floral bud development mechanisms.

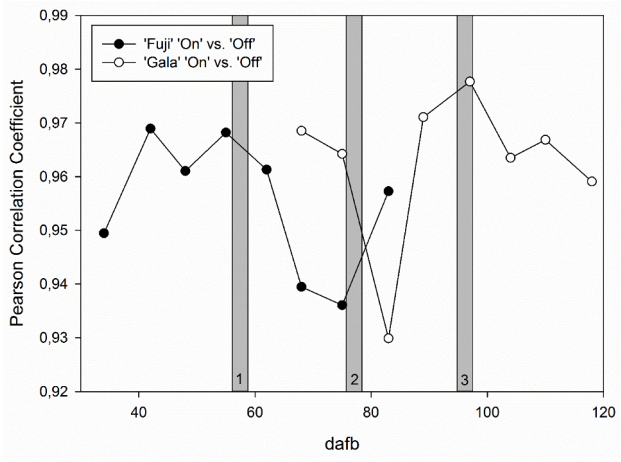

Fig. 7. Pearson correlation coefficients between proteomic profiles of buds from 'On' and 'Off' trees. Grey bars indicate the calculated onset of bud initiation in 'Off' trees based on histological data [23] for 'Fuji' (1) and 'Gala' (2) at 57 and 76 dafb, respectively, and for 'Gala' 'On' trees (3) at 96 dafb. No starting point of bud initiation could be calculated for 'Fuji' 'On' due to a lack of initiated buds.

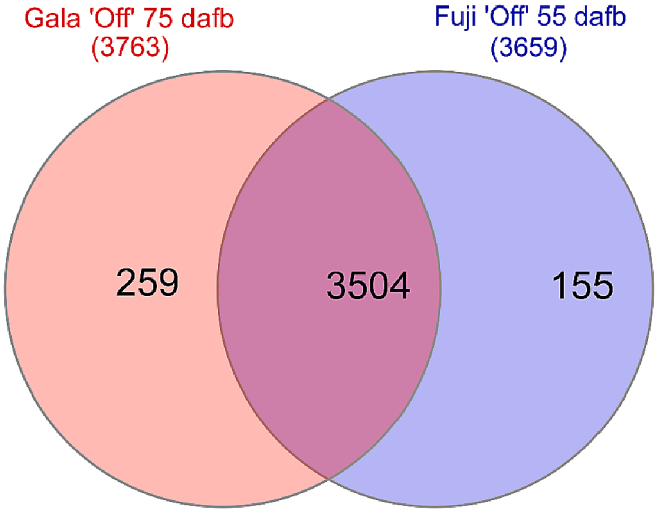

Fig. 8. Venn diagram of identified proteins in buds from 'Gala' 'Off' at 75 dafb and 'Fuji' 'Off' at 55 dafb that were used for the cultivar comparison.

3.4. The phenylpropanoid and flavonoid pathway

Key proteins of the phenylpropanoid and flavonoid pathways such as PAL1, C4H, F3H, LDOX showed lower abundances in buds from 'On' trees in both cultivars (except C4H in 'Fuji'). The identified proteins are illustrated in Fig. 9.

One of the products of the phenylpropanoid pathway, chlorogenic acid, is correlated with the expression of PAL [59]. It is reported, that chlorogenic acid inhibits the activity of indole-3-acetic acid-oxidase and thereby maintains the active form of auxin [60], a plant hormone, that, at low concentrations, encouraged bud formation in *Plumbago indica* [61].

4. Conclusion

The results of this study highlight several mechanisms possibly involved in early floral bud development, during bud initiation, in apple on a proteomic level. We have identified several proteins, that show different abundances in apple buds over the period of flower bud

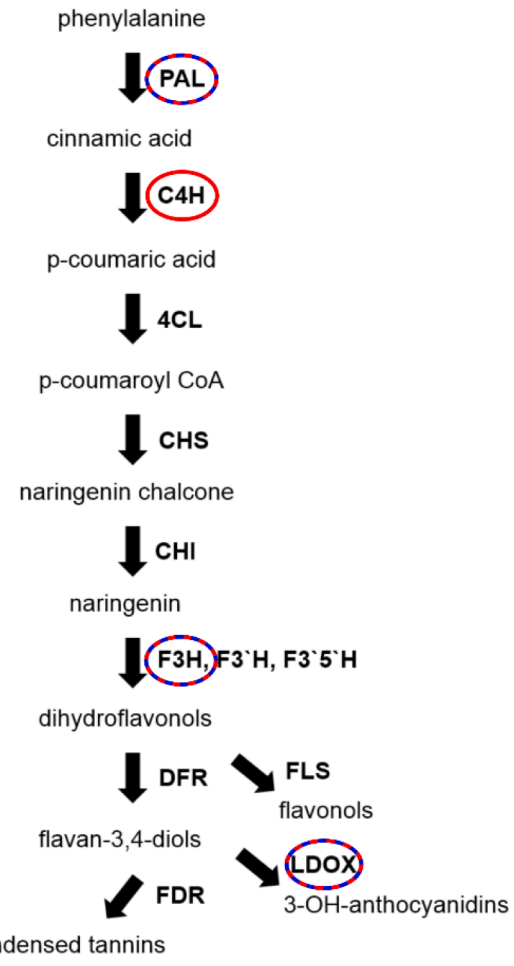

Fig. 9. Schematic phenylpropanoid and flavonoid pathways, adapted from Winkel-Shirley [52]. Enzymes found in 'Gala' are marked in red, enzymes found in 'Fuji' are marked in blue. PAL, phenylalanine ammonia-lyase; C4H, trans-cinnamate 4-monooxygenase; 4CL, 4-coumaroyl:CoA ligase; CHS, chalcone synthase; CHI, chalcone isomerase; F3H, Naringenin,2-oxoglutarate 3-dioxygenase; F3`H and F3`5′H, flavonoid 3` and 3`5` hydroxylase; DFR, dihydroflavonol 4-reductase; FLS, flavonol synthase; FDR, flavan-3,4-diol reductase; LDOX, leucoanthocyanidin dioxygenase. Not shown is CCOAMT, caffeoyl-CoA *O*-methyltransferase. (For interpretation of the references to colour in this figure legend, the reader is referred to the web version of this article.)

initiation. Furthermore, proteins were identified that possibly contribute to the differences in floral bud development of apple cultivars with regular and alternate bearing behavior. These results may lay the foundation for future development of biomarkers, that help determine the degree of alternate bearing behavior early in breeding programs to select for more regular bearing cultivars.

Firstly, the lower abundance of key proteins of the phenylpropanoid and flavonoid pathway, specifically the reduced abundance of PAL, could lead to less active auxin because of the reduced production of chlorogenic acid and thereby inhibiting flower bud formation as explained in chapter 3.4. Future metabolic studies on buds from 'On' and 'Off' trees could further evaluate this hypothesis by determining the content of metabolites such as chlorogenic acid in the buds. Secondly, ferritins increased in 'On' buds from 'Gala' and 'Fuji' trees. The iron-storage proteins [62] apparently play an essential role in building up enough iron storage capacities to enable vigorous vegetative growth [48]. Thirdly, the higher abundance of the histone deacetylase MD11G1156500 in buds from 'Gala' 'On' trees compared to 'Off' trees supports the hypothesis, that histone modification plays an essential role

during flower initiation also in apple, a result that so far was described for *Arabidopsis thaliana* [55,63], apple [21] and rice [64]. The presence of S-adenosylmethionine synthetases in 'Fuji' 'Off' buds indicate that histone and DNA methylation could possibly be involved in the flower bud induction process [43]. However, further epigenomic studies are necessary to confirm a causal relationship.

Funding

This research was financially supported by the Deutsche Forschungsgemeinschaft (WU 584/7-1) and by Horticulture Innovation Australia Limited (AP15002).

Author contribution statement

JK, AM, HF and JW conceptualized and conducted the experiment; BW carried out the MS analysis; JP assisted in the statistical evaluation of the dataset; JK wrote the first draft of the manuscript; AM wrote sections of the manuscript; JW, HF and JP critically revised the manuscript. All authors read and approved the manuscript.

Declaration of Competing Interest

The authors declare no competing interests.

Data availability

Annex 3 contains all Log2(x) transformed LFQ intensities of the 4020 identified proteins in 96 bud samples (2 cultivars, 2 treatments, 8 time points, 3 replicates).

Acknowledgements

The authors thank the staff of the Institute of Crop Science, Department of Crop Physiology of Specialty Crops (340f), University of Hohenheim, for assistance during the sampling periods. This research was financially supported by the Deutsche Forschungsgemeinschaft (WU 584/7-1) and by Horticulture Innovation Australia Limited (AP15002).

Appendix A. Supplementary data

Supplementary data to this article can be found online at https://doi.org/10.1016/j.jprot.2021.104459.

References

[1] S. Tamaki, S. Matsuo, L.H. Wong, S. Yokoi, K. Shimamoto, Hd3a protein is a mobile flowering signal in rice, Science (80-.) 316 (2007) 1033–1036, https://doi.org/10.1126/science.1141753.
[2] F. Valverde, A. Mouradov, W. Soppe, D. Ravenscroft, A. Samach, G. Coupland, Photoreceptor regulation of constans protein in photoperiodic flowering by science 2004 photoperiodism : monitoring day length in arabidopsis, Science (80-.) 2 (2007) 1003–1007.
[3] W. Mahrez, J. Shin, R. Muñoz-Viana, D.D. Figueiredo, M.S. Trejo-Arellano, V. Exner, A. Siretskiy, W. Gruissem, C. Köhler, L. Hennig, BRR2a Affects Flowering Time via FLC Splicing, PLoS Genet. 12 (2016) 1–25, https://doi.org/10.1371/journal.pgen.1005924.
[4] L. Corbesier, C. Vincent, S. Jang, F. Fornara, Q. Fan, I. Searle, A. Giakountis, S. Farrona, L. Gissot, C. Turnbull, G. Coupland, FT protein movement contributes to long-distance signaling in floral induction of Arabidopsis, Science (80-.) 316 (2007) 1030–1033, https://doi.org/10.1126/science.1141752.
[5] P.A. Wigge, FT, a mobile developmental signal in plants, Curr. Biol. 21 (2011), https://doi.org/10.1016/j.cub.2011.03.038.
[6] T. Buban, M. Faust, Flower bud induction in apple trees: internal control and differentiation, in: J. Janick (Ed.), Hortic. Rev vol. 4, John Wiley & Sons, Westport, 1982, pp. 174–203. http://onlinelibrary.wiley.com/doi/10.1002/9781118060773.ch6/summary.
[7] C. Hättasch, H. Flachowsky, D. Kapturska, M.-V. Hanke, Isolation of flowering genes and seasonal changes in their transcript levels related to flower induction and initiation in apple (*Malus domestica*), Tree Physiol. 28 (2008) 1459–1466, https://doi.org/10.1093/treephys/28.10.1459.
[8] M.-V. Hanke, H. Flachowsky, A. Peil, C. Hättasch, No flower no fruit – genetic potentials to trigger flowering in fruit trees, Genes, Genomes and Genomics. 1 (2007) 1–20.
[9] N. Koutinas, G. Pepelyankov, V. Lichev, Flower induction and flower bud development in apple and sweet cherry, Biotechnol. Biotechnol. Equip. 24 (2010) 1549–1558, https://doi.org/10.2478/V10133-010-0003-9.
[10] R.M. Fulford, The morphogenesis of apple Buds: II. The development of the bud, Ann. Bot. 30 (1966) 25–38. http://aob.oxfordjournals.org/content/30/4/597.abstract.
[11] T. Foster, R. Johnston, A. Seleznyova, A morphological and quantitative characterization of early floral development in apple (Malus x domestica Borkh.), Ann. Bot. 92 (2003) 199–206, https://doi.org/10.1093/aob/mcg120.
[12] J.D. Wilkie, M. Sedgley, T. Olesen, Regulation of floral initiation in horticultural trees, J. Exp. Bot. 59 (2008) 3215–3228, https://doi.org/10.1093/jxb/ern188.
[13] J. Tromp, Flower-bud formation in pome fruits as affected by fruit thinning, Plant Growth Regul. 31 (2000) 27–34, https://doi.org/10.1023/a:1006342328724.
[14] H. Jonkers, Biennial bearing in apple and pear: a literature survey, Sci. Hortic. (Amsterdam). 11 (1979) 303–317.
[15] M.W. Williams, L.J. Edgerton, Fruit thinning of apples and pears with chemicals, in: Rev., Agric. Inf. Bull. No. 289 - US Dept. Agric, 1981.
[16] C. Pratt, Apple flower and fruit: morphology and anatomy, in: J. Janick (Ed.), Hortic. Rev vol. 10, John Wiley & Sons, Hoboken, 1988, pp. 273–308.
[17] F.G. Dennis, J.C. Neilsen, Physiological factors affecting biennial bearing in tree fruit: the role of seeds in apple, Horttechnology. 9 (1999) 317–322. http://horttech.ashspublications.org/content/9/3/317.short.
[18] X. Zuo, D. Zhang, S. Wang, L. Xing, Y. Li, S. Fan, L. Zhang, J. Ma, C. Zhao, K. Shah, N. An, M. Han, Expression of genes in the potential regulatory pathways controlling alternate bearing in 'Fuji' (*Malus domestica* Borkh.) apple trees during flower induction, Plant Physiol. Biochem. 132 (2018) 579–589, https://doi.org/10.1016/j.plaphy.2018.10.003.
[19] Y. Li, D. Zhang, X. Zhang, L. Xing, S. Fan, J. Ma, C. Zhao, L. Du, M. Han, A transcriptome analysis of two apple (Malus × domestica) cultivars with different flowering abilities reveals a gene network module associated with floral transitions, Sci. Hortic. (Amsterdam). 239 (2018) 269–281, https://doi.org/10.1016/j.scienta.2018.04.048.
[20] Y. Li, D. Zhang, N. An, S. Fan, X. Zuo, X. Zhang, L. Zhang, C. Gao, M. Han, L. Xing, Transcriptomic analysis reveals the regulatory module of apple (Malus × domestica) floral transition in response to 6-BA, BMC Plant Biol. 19 (2019) 1–17, https://doi.org/10.1186/s12870-019-1695-0.
[21] S. Fan, J. Wang, C. Lei, C. Gao, Y. Yang, Y. Li, N. An, D. Zhang, M. Han, Identification and characterization of histone modification gene family reveal their critical responses to flower induction in apple, BMC Plant Biol. 18 (2018) 173, https://doi.org/10.1186/s12870-018-1388-0.
[22] S. Fan, X. Gao, C. Gao, Y. Yang, X. Zhu, W. Feng, R. Li, M. Mobeen Tahir, D. Zhang, M. Han, N. An, Dynamic Cytosine DNA Methylation Patterns Associated with mRNA and siRNA Expression Profiles in Alternate Bearing Apple Trees, J. Agric. Food Chem. 67 (2019) 5250–5264, https://doi.org/10.1021/acs.jafc.9b00871.
[23] J. Kofler, A. Milyaev, F. Capezzone, S. Stojnić, N. Mićić, H. Flachowsky, M. V. Hanke, J.N. Wünsche, High crop load and low temperature delay the onset of bud initiation in apple, Sci. Rep. 9 (2019) 11, https://doi.org/10.1038/s41598-019-54381-x.
[24] A. Milyaev, J. Kofler, J. Pfannstiel, D. Stefanelli, H. Flachowsky, M.V. Hanke, J. N. Wünsche, Histological and proteomic approaches to study floral bud induction in relation to biennial bearing in apple, Acta Hortic. 1229 (2018), https://doi.org/10.17660/ActaHortic.2018.1229.42.
[25] M. Afzal, J. Pfannstiel, J. Zimmermann, S.C. Bischoff, T. Würschum, C.F.H. Longin, High-resolution proteomics reveals differences in the proteome of spelt and bread wheat flour representing targets for research on wheat sensitivities, Sci. Rep. 10 (2020) 1–11, https://doi.org/10.1038/s41598-020-71712-5.
[26] C.L. Kielkopf, W. Bauer, I.L. Urbatsch, Bradford assay for determining protein concentration, Cold Spring Harb. Protoc. 2020 (2020) 136–138, https://doi.org/10.1101/pdb.prot102269.
[27] S. Saveliev, M. Bratz, R. Zubarev, M. Szapacs, H. Budamgunta, M. Urh, Trypsin/Lys-C protease mix for enhanced protein mass spectrometry analysis, Nat. Methods. 10 (2013), https://doi.org/10.1038/nmeth.f.371.
[28] J. Rappsilber, Y. Ishihama, M. Mann, Stop and go extraction tips for matrix-assisted laser desorption/ionization, nanoelectrospray, and LC/MS sample pretreatment in proteomics, Anal. Chem. 75 (2003) 663–670, https://doi.org/10.1021/ac026117i.
[29] J.V. Olsen, L.M.F. de Godoy, G. Li, B. Macek, P. Mortensen, R. Pesch, A. Makarov, O. Lange, S. Horning, M. Mann, Parts per Million Mass Accuracy on an Orbitrap Mass Spectrometer via Lock Mass Injection into a C-trap, Mol. Cell. Proteomics. 4 (2005) 2010–2021, https://doi.org/10.1074/mcp.T500030-MCP200.
[30] J. Cox, M. Mann, MaxQuant enables high peptide identification rates, individualized p.p.b.-range mass accuracies and proteome-wide protein quantification, Nat. Biotechnol. 26 (2008) 1367–1372, https://doi.org/10.1038/nbt.1511.
[31] N. Daccord, J.-M. Celton, G. Linsmith, C. Becker, N. Choisne, E. Schijlen, H. van de Geest, L. Bianco, D. Micheletti, R. Velasco, E.A. Di Pierro, J. Gouzy, D.J.G. Rees, P. Guérif, H. Muranty, C.-E. Durel, F. Laurens, Y. Lespinasse, S. Gaillard, S. Aubourg, H. Quesneville, D. Weigel, E. van de Weg, M. Troggio, E. Bucher, High-quality de novo assembly of the apple genome and methylome dynamics of early fruit development, Nat. Genet. 49 (2017) 1099–1106, https://doi.org/10.1038/ng.3886.
[32] S. Tyanova, T. Temu, P. Sinitcyn, A. Carlson, M.Y. Hein, T. Geiger, M. Mann, J. Cox, The Perseus computational platform for comprehensive analysis of (prote)

omics data, Nat. Methods. 13 (2016) 731–740, https://doi.org/10.1038/nmeth.3901.
[33] Z. Pang, J. Chong, G. Zhou, D.A. De Lima Morais, L. Chang, M. Barrette, C. Gauthier, P.É. Jacques, S. Li, J. Xia, MetaboAnalyst 5.0: Narrowing the gap between raw spectra and functional insights, Nucleic Acids Res. 49 (2021) W388–W396, https://doi.org/10.1093/nar/gkab382.
[34] A.P. Diz, A. Carvajal-Rodríguez, D.O.F. Skibinski, Multiple hypothesis testing in proteomics: a strategy for experimental work, Mol. Cell. Proteomics. 10 (2011), https://doi.org/10.1074/mcp.M110.004374.
[35] S. Rosenfeld, T. Wang, Y. Kim, J. Milner, Numerical deconvolution of cDNA microarray signal, Ann. N. Y. Acad. Sci. 1020 (2004) 110–123, https://doi.org/10.1196/annals.1310.012.
[36] H. Ogata, S. Goto, K. Sato, W. Fujibuchi, H. Bono, M. Kanehisa, KEGG: Kyoto encyclopedia of genes and genomes, Nucleic Acids Res. 27 (1999) 29–34, https://doi.org/10.1093/nar/27.1.29.
[37] D. Szklarczyk, A.L. Gable, D. Lyon, A. Junge, S. Wyder, J. Huerta-Cepas, M. Simonovic, N.T. Doncheva, J.H. Morris, P. Bork, L.J. Jensen, C. Von Mering, STRING v11: Protein-protein association networks with increased coverage, supporting functional discovery in genome-wide experimental datasets, Nucleic Acids Res. 47 (2019) D607–D613, https://doi.org/10.1093/nar/gky1131.
[38] S. Brohée, J. van Helden, Evaluation of clustering algorithms for protein-protein interaction networks, BMC Bioinformatics. 7 (2006), https://doi.org/10.1186/1471-2105-7-488.
[39] P.-É. Lauri, G. Bourdel, C. Trottier, H. Cochard, Apple shoot architecture: evidence for strong variability of bud size and composition and hydraulics within a branching zone, New Phytol. 178 (2008) 798–807, https://doi.org/10.1111/j.1469-8137.2008.02416.x.
[40] F.B. Pichler, E.F. Walton, M. Davy, C. Triggs, B. Janssen, J.N. Wünsche, J. Putterill, R.J. Schaffer, Relative developmental, environmental, and tree-to-tree variability in buds from field-grown apple trees, Tree Genet. Genomes. 3 (2007) 329–339, https://doi.org/10.1007/s11295-006-0073-x.
[41] A. Zhou, H. Sun, S. Dai, S. Feng, J. Zhang, S. Gong, J. Wang, Identification of Transcription Factors Involved in the Regulation of Flowering in Adonis Amurensis Through Combined RNA-seq Transcriptomics and iTRAQ Proteomics, Genes (Basel). 10 (2019).
[42] Y.D. Bi, Z.G. Wei, Z. Shen, T.C. Lu, Y.X. Cheng, B.C. Wang, C.P. Yang, Comparative temporal analyses of the *Pinus sylvestris* L. var. mongolica litv. apical bud proteome from dormancy to growth, Mol. Biol. Rep. 38 (2011) 721–729, https://doi.org/10.1007/s11033-010-0159-2.
[43] W. Li, Y. Han, F. Tao, K. Chong, Knockdown of SAMS genes encoding S-adenosyl-l-methionine synthetases causes methylation alterations of DNAs and histones and leads to late flowering in rice, J. Plant Physiol. 168 (2011) 1837–1843, https://doi.org/10.1016/j.jplph.2011.05.020.
[44] L.A. Wanner, G. Li, D. Ware, I.E. Somssich, K.R. Davis, The phenylalanine ammonia-lyase gene family in *Arabidopsis thaliana*, Plant Mol. Biol. 27 (1995) 327–338, https://doi.org/10.1007/BF00020187.
[45] A. Erez, S. Lavee, Prunin identification, biological activity and quantitative change in comparison to naringenin in dormant peach buds, Plant Physiol. 44 (1969) 342–346, https://doi.org/10.1104/pp.44.3.342.
[46] S. Abrahams, E. Lee, A.R. Walker, G.J. Tanner, P.J. Larkin, A.R. Ashton, The Arabidopsis TDS4 gene encodes leucoanthocyanidin dioxygenase (LDOX) and is essential for proanthocyanidin synthesis and vacuole development, Plant J. 35 (2003) 624–636, https://doi.org/10.1046/j.1365-313X.2003.01834.x.
[47] T. Yang, B.W. Poovaiah, Calcium/calmodulin-mediated signal network in plants, Trends Plant Sci. 8 (2003) 505–512, https://doi.org/10.1016/j.tplants.2003.09.004.
[48] K. Ravet, B. Touraine, J. Boucherez, J.F. Briat, F. Gaymard, F. Cellier, Ferritins control interaction between iron homeostasis and oxidative stress in Arabidopsis, Plant J. 57 (2009) 400–412, https://doi.org/10.1111/j.1365-313X.2008.03698.x.
[49] B. Chrost, U. Kolukisaoglu, B. Schulz, K. Krupinska, An α-galactosidase with an essential function during leaf development, Planta 225 (2007) 311–320, https://doi.org/10.1007/s00425-006-0350-9.
[50] D. Zilberman, X. Cao, S.E. Jacobsen, ARGONAUTE4 control of locus-specific siRNA accumulation and DNA and histone methylation, Science (80-.) 299 (2003) 716–719, https://doi.org/10.1126/science.1079695.
[51] D. Guo, F. Chen, K. Inoue, J.W. Blount, R.A. Dixon, Downregulation of caffeic acid 3-O-methyltransferase and caffeoyl CoA 3-O-methyltransferase in transgenic alfalfa: Impacts on lignin structure and implications for the biosynthesis of G and S lignin, Plant Cell. 13 (2001) 73–88, https://doi.org/10.1105/tpc.13.1.73.
[52] B. Winkel-Shirley, Evidence for enzyme complexes in the phenylpropanoid and flavonoid pathways, Physiol. Plant. 107 (1999) 142–149, https://doi.org/10.1034/j.1399-3054.1999.100119.x.
[53] G. Böhmdorfer, M.J. Rowley, J. Kuciński, Y. Zhu, I. Amies, A.T. Wierzbicki, RNA-directed DNA methylation requires stepwise binding of silencing factors to long non-coding RNA, Plant J. 79 (2014) 181–191, https://doi.org/10.1111/tpj.12563.
[54] C. Xia, Y.J. Wang, W.Q. Li, Y.R. Chen, Y. Deng, X.Q. Zhang, L.Q. Chen, D. Ye, The Arabidopsis eukaryotic translation initiation factor 3, subunit F (AteIF3f), is required for pollen germination and embryogenesis, Plant J. 63 (2010) 189–202, https://doi.org/10.1111/j.1365-313X.2010.04237.x.
[55] Y. He, S.D. Michaels, R.M. Amasino, Regulation of flowering time by histone acetylation in arabidopsis, Science (80-.) 302 (2003) 1751–1754, https://doi.org/10.1126/science.1091109.
[56] R. Yano, Y. Takebayashi, E. Nambara, Y. Kamiya, M. Seo, Combining association mapping and transcriptomics identify HD2B histone deacetylase as a genetic factor associated with seed dormancy in *Arabidopsis thaliana*, Plant J. 74 (2013) 815–828, https://doi.org/10.1111/tpj.12167.
[57] S.L. Berger, The complex language of chromatin regulation during transcription, Nature 447 (2007) 407–412, https://doi.org/10.1038/nature05915.
[58] M. Delseny, N. Bies-etheve, C. Carles, G. Hull, C. Vicient, M. Raynal, F. Grellet, Late Embryogenesis Abundant (LEA) protein gene regulation during Arabidopsis seed maturation, J. Plant Physiol. 427 (2001) 419–427.
[59] R.S. Payyavula, R. Shakya, V.G. Sengoda, J.E. Munyaneza, P. Swamy, D. A. Navarre, Synthesis and regulation of chlorogenic acid in potato: Rerouting phenylpropanoid flux in HQT-silenced lines, Plant Biotechnol. J. 13 (2015) 551–564, https://doi.org/10.1111/pbi.12280.
[60] P.E. Pilet, Effect of chlorogenic acid on the auxin catabolism and the auxin content of root tissues, Phytochemistry. 3 (1964) 617–621, https://doi.org/10.1016/S0031-9422(00)82937-4.
[61] C. Nitsch, J.P. Nitsch, The induction of flowering in vitro in stem segments of *Plumbago indica* L, Planta 72 (1967) 371–384, https://doi.org/10.1007/bf00390147.
[62] J.F. Briat, Roles of ferritin in plants, J. Plant Nutr. 19 (1996) 1331–1342, https://doi.org/10.1080/01904169609365202.
[63] W. Kim, D. Latrasse, C. Servet, D.X. Zhou, Arabidopsis histone deacetylase HDA9 regulates flowering time through repression of AGL19, Biochem. Biophys. Res. Commun. 432 (2013) 394–398, https://doi.org/10.1016/j.bbrc.2012.11.102.
[64] J. Shi, A. Dong, W.H. Shen, Epigenetic regulation of rice flowering and reproduction, Front, Plant Sci. 5 (2015) 1–13, https://doi.org/10.3389/fpls.2014.00803.